International Journal of Applied Science and Engineering Review

IJASER

ISSN: 2582-6271

Vol. 3, Issue.2, March-April 2022, page no. 32-43

To cite this article: Asotah Wisdom, Onuoha Chukwudike, Medupin Olawale and Elakhame Zeberu (2022). IMPLEMENTATION OF EXPERIMENTAL DESIGN IN EVALUATING THE MECHANICAL PROPERTIES OF CERAMIC COMPOSITES, International Journal of Applied Science and Engineering Review (IJASER) 3 (2): 32-43

IMPLEMENTATION OF EXPERIMENTAL DESIGN IN EVALUATING THE MECHANICAL PROPERTIES OF CERAMIC COMPOSITES

Asotah Wisdom[1]*, Onuoha Chukwudike[1], Medupin Olawale[1] and Elakhame Zeberu[2]

[1]Department of Materials and Metallurgical Engineering, Federal University of Technology Owerri, PMB 1526, Owerri, Imo State, Nigeria

[2]Federal Institute of Industrial Research Oshodi, Lagos State, Nigeria

DOI: http://dx.doi.org/10.52267/IJASER.2022.3203

ABSTRACT

The influence of independent variables (firing temperature and residue content) on mechanical properties – hardness, compressive strength, flexural strength, compression modulus and energy at the break – of ceramic composites was investigated through experimental design. Microstructural evaluation using scanning electron microscopy (SEM) and mineralogical identification using x-ray diffraction (XRD) was also accomplished to understand the structure-property relationship. In analysing the observed data, variance analysis was employed to determine the statistical significance of the factors on the responses and regression equations showing correlations were developed. The observed data were shown to accept the null hypothesis for hardness, compression modulus and compressive strength, while flexural strength and energy at break rejected the null hypothesis judging by the p-value. The flexural strength showed a good correlation, but the influence of firing temperature and residue was minimal. However, both factors' square was shown to influence the flexural strength considerably. The study presents a systematic way to understand causal relationships, ensuring that product specifications and quality are met.

KEYWORDS: Ceramics, Central Composite Design, Response Surface, Compressive Strength, Optimisation

1. INTRODUCTION

Computer modelling is fast changing how research is carried out worldwide, primarily because multivariable experimentation is complex, time-consuming and expensive. Therefore, computers are being used to mathematically design and model the system to understand how different variables affect the system and predict the behaviour under certain conditions (Sacks et. al., 1989). Computer

ISSN: 2582-6271

Vol. 3, Issue.2, Mar-Apr 2022, page no. 32-43

modelling of experimental conditions can help better process control, thereby improving the final product/process (Sundarkrishnaa, 2015; Abtew et al., 2018).

For ceramic manufacturing, where different input materials are used alongside traditional materials, the onus lies on the researcher/manufacturer to understand how these materials affect the processing conditions, route and final products. Consequent to the natural tolerance of ceramics for different materials in its production, researchers now rely on statistical analysis and computer modelling to better understand its products' structure, processing, properties, and performance relationship (Silva et al., 2018).

One of such tools is the use of the design of experiments (DOE) which has significant advantages over the "one factor at a time" (OFAT) technique. DOE allows the researcher to simultaneously vary the variables, reducing the number of experiments done, thereby saving time and cost (Ogunbiyi, 2018; Levinson, 2017).

Adopting experimental design, Silva et al. (2018) incorporated quartzite residues in porcelain tiles production, modelled and optimised the effect of firing temperature and residue content on the dependent variables (linear shrinkage, water absorption, apparent density and flexural strength). However, quartzite particles have been noted to induce cracks due to the α-β phase transformation at 573oC (Abeid & Park, 2018). It leaves a gap in the literature that some researchers have attempted to fill.

Chukwudi et al., (2012) used slag, a by-product of iron smelting, to replace quartz, while Quaranta et al., (2014) opted for metallurgical wastes. Other researchers have also used industrial and agricultural wastes to replace quartz in the body of triaxial ceramics, (Correia et al., 2009; De Silva and Surangi, 2017; Haile et al., 2019) with different levels of success achieved. After replacing quartzite with steel slag, Correia et al., (2009), found that the samples containing between 20 – 60% of slag had good qualities for application as floor tiles. However, another attempt by Haile et al., (2019), using waste plastic bottles, showed that the composite could only tolerate up to 32.11% of waste plastic in its matrix. At the same time, Silva et al., (2017), attempt using agate reject had a tolerance of 15 – 22%.

Notwithstanding these efforts made along this line of inquiry, this present study aims to contribute to on-going efforts in literature, applying experimental techniques against traditional OFAT techniques within a firing range of 1000 – 1100○C. This study, cognizant of the deleterious effect of quartz particles, will replace quartz with rice husk ash. Central composite design (CCD) type of

International Journal of Applied Science and Engineering Review

IJASER

ISSN: 2582-6271

Vol. 3, Issue.2, Mar-Apr 2022, page no. 32-43

response surface method will be adopted to determine the effect of firing temperature and residue content on the mechanical properties of manufactured ceramic tiles. Also, regression equations showing the effect of the independent variables as a function of the dependent variables will be generated and data generated analysed using variance analysis.

2. Experimental Procedure

The raw materials used in this study were: kaolin, feldspar, and rice husk ash (RHA). The kaolin and feldspar were sourced from Ogun State, Nigeria, while the rice husk was collected in Lagos, Nigeria. The rice husk was burnt to ashes and sieved to produce the rice husk ash (RHA). The clay was soaked for 24 hours and sieved with a mesh of 150 µm. After that, particles such as sand silt with a diameter greater than 150 µm disposed of as impurities. In an attempt to obtain a fine powder, the wet clay was air-dried and further milled in a ball mill (Model 87002 Limongs – France A50 – 43). After that, feldspar rock was crushed and milled to particle size less than 150 µm. The ash produced from the burnt rice husk was also sieved to particle size less than 150 µm. All particle size analysis was done using standard sieve BS 410. Table 1 presents the analysed factors within the range considered.

Table 1: Firing temperature, residue content and their levels and coded values

LEVELS	- √2	-1	0	+1	+√2
FACTORS					
FT (ºC)	1030	1040	1065	1090	1100
RC (%)	5.85	10	20	30	34.12

To determine the correlation between the independent variables and the dependent variable, the Central Composite Design type Response Surface Method was used. The design produced using Minitab 19 Statistical Software consisted of two factors (firing temperature (FT) and residue content (% RHA)), which gave five centre points, four axial points and four cube points. The particles were measured using a weighing balance of 0.001 mg accuracy, and water was added to aid mixture homogeneity and workability. After a quantity of composite paste was placed in a mould and on the mantelpiece of the hydraulic press, then a minimum pressure of 300 KN/m2 was applied uniaxial. Prior to compaction, the mould was sufficiently lubricated to aid the removal of the specimen. The compacted composite was dried in an oven (Memmert GmbH, Germany) at 90 – 100 ºC. Specimens were then fired at the rate of 5˚C/min between 1000 ˚C and 1100 ˚C in an electric furnace (Thermolyne 46200). The process chart is shown in Figure 1.

International Journal of Applied Science and Engineering Review

IJASER

ISSN: 2582-6271

Vol. 3, Issue.2, Mar-Apr 2022, page no. 32-43

Figure 1: Flow chart showing process methodology

3. Mechanical Property Tests

Hardness, compressive strength, compression modulus, flexural strength, and energy at break were evaluated. The resistance to indentation (hardness) was carried out using a hardness testing machine (Model RBHT, Serial Number 2011/202) on Rockwell scale B, using a load of 100 kg and steel ball indenter with 1/16-inch diameter. Compressive strength and compression modulus were determined using the Instron Testing Machine (Model 3369) according to ASTM C39/ C 39M – 03 standards. Compressive axial load was applied on the test specimens until fracture, and the maximum load divided by the specimen's cross-sectional area was evaluated for compressive strength. Load displacement plots were obtained on an x-y axis, and compressive strain at maximum compressive stress was obtained from the plot (Fig. 2).

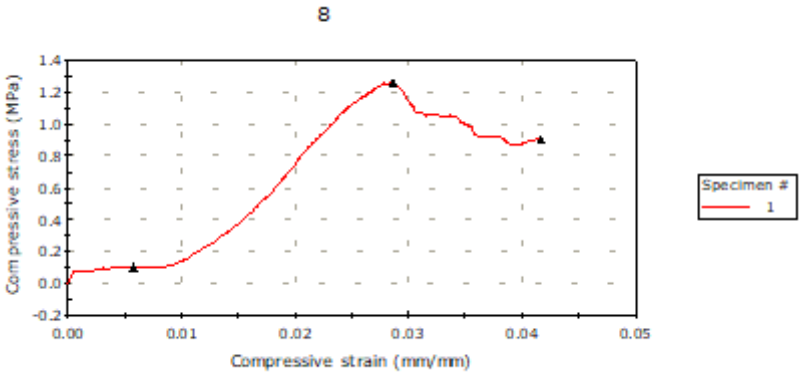

(a)

International Journal of Applied Science and Engineering Review

IJASER

ISSN: 2582-6271

Vol. 3, Issue.2, Mar-Apr 2022, page no. 32-43

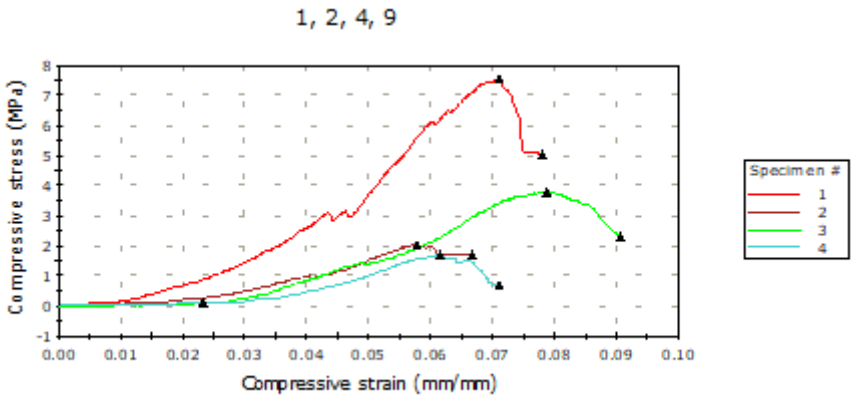

(b)

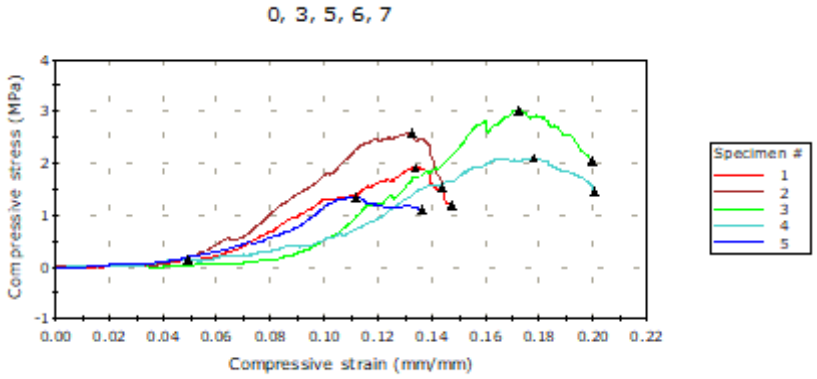

(c)

Figure 2: Plot showing compressive stress at strain for specimens

It was used to determine the compression modulus. The plot also deduced the maximum energy absorbed by the specimen under compression before fracture, which is a measure of toughness. Materials reaction to bending stress known as flexural strength was also determined using the Ametek EX 250 Digital Compression and Tension tester by subjecting the specimen to a three-point bend test until the specimen fractured. Scanning Electron Microscopy (Phenom ProX SEM) technique investigated the specimen structure and elemental composition while the mineralogical phases were analysed using X-ray diffraction (Rigaku Miniflex X-ray Diffractometer).

4. RESULT AND DISCUSSION

ISSN: 2582-6271

Vol. 3, Issue.2, Mar-Apr 2022, page no. 32-43

Table 2 presents the value of the observed mechanical properties, namely: HRB (Rockwell Hardness B), CS (Compressive Strength), E–MOD (Compressive Elastic Modulus), FS (Flexural Strength) and E – BRK (Energy at Break) derived from the experimental runs generated using Minitab 19 software against values predicted by the mathematical model. The data sets (Table 2) show limited variability between the observed and model-predicted values. Table 3 shows the variance analysis of fitted responses. From the table, P-value was used to determine a relationship between the sampled observed responses and the population.

At P-value < 0.05, the observed responses were determined for statistical significance, which means a 95% chance that the responses of the selected sample reflected in the population are not due to chance (Dahiru, 2011). As observed from Table 3, HRB, CS and E – MOD models do not represent the population, and the factors considered do not statistically influence the mechanical properties within the range investigated. It can be attributed to the lack of mullite phase formation within the firing range (Figure 3). Other researchers have observed that the dependent variables investigated in this research improve significantly when its synthesis and subsequent firing are done above the mullitisation temperature (Aksel, 2003; Anggono, 2005). According to Ban and Okada (1994), the mullitisation temperature is when mullite crystals are expected to form and falls above 1200 ºC. Therefore, the temperature range (1030˚C - 1100˚C) considered in this study is insufficient to improve mechanical properties.

Table 2: Observed and Predicted Mechanical Values

FS (MPa)		E-BRK (J)		E-MOD (MPa)		CS (MPa)		HRB	
Observed	Predicted	Observed	Predicted	Observed	Predicted	Observed	Predicted	Observed	Predicted
1.258	1.107	5.340	4.001	0.1766	0.0926	3.037	2.148	43.100	46.980
1.568	1.568	0.710	0.710	0.4412	0.4412	1.262	1.262	45.400	45.400
0.992	1.109	3.710	5.059	0.1946	0.4234	2.577	4.316	48.600	43.859
1.568	1.568	0.710	0.710	0.4412	0.4412	1.262	1.262	45.400	45.400
1.021	1.180	1.870	3.011	0.1205	0.0859	1.350	1.498	49.000	46.031

ISSN: 2582-6271

Vol. 3, Issue.2, Mar-Apr 2022, page no. 32-43

1.425	1.285	4.310	3.418	0.1179	0.1752	2.099	2.147	37.650	40.185
1.098	1.200	2.670	3.397	0.1429	0.1719	1.915	2.328	44.400	41.565
1.043	0.974	2.940	2.194	0.4837	0.3099	3.803	2.593	47.050	50.743
0.840	0.899	1.170	2.106	0.3525	0.6448	2.037	4.041	58.250	53.644
1.568	1.568	0.710	0.710	0.4412	0.4412	1.262	1.262	45.400	45.400
1.568	1.568	0.710	0.710	0.4412	0.4412	1.262	1.262	45.400	45.400
1.568	1.568	0.710	0.710	0.4412	0.4412	1.262	1.262	45.400	45.400
1.102	1.022	5.140	3.953	1.0632	0.7482	7.552	5.351	42.150	47.190

The observed data is fitted to the model, and the regression equation showing the dependent variable (mechanical properties) as a function of the independent variables (firing temperature and residue content) are shown in Equations 1-5. The corresponding regression coefficients and model adequacy predictors: R2 (R-squared) and R2 – adjusted (R – squared adjusted) are also shown in Table 3.

Table 3: Relevant Statistics for Analysis of Variance of Mathematical Models that Describes the Variables: HRB, CS, FS, E-MOD and E – BRK

Response	Model	F-value	P-value	R^2	R^2-adjusted
HRB	Quadratics	1.65	0.263	0.54	0.21
CS	Quadratics	2.18	0.17	0.61	0.33
FS	Quadratics	10.46	0.004	0.88	0.8
E-MOD	Quadratics	2.43	0.139	0.63	0.37
E-BRK	Quadratics	4.46	0.038	0.76	0.59

International Journal of Applied Science and Engineering Review

IJASER

ISSN: 2582-6271

Vol. 3, Issue.2, Mar-Apr 2022, page no. 32-43

Key: FS = Flexural Strength; E-BRK= Energy at Break; C = Compressive Strength; E-MOD = Compression Elastic Modulus; HRB = Rockwell Hardness

Notwithstanding, dependent variables E – BRK and FS rejected the null hypothesis and showed statistical significance over the range investigated. The regression equations (Equation 1 – 5) show that decreasing the firing temperature will increase hardness, compressive strength, and energy at the break. However, the model prediction does not agree with Silva et al., (2018), who argued that increasing firing temperature favours the more significant formation of the liquid phase, facilitating densification, which improves the hardness, compressive strength and compression modulus. The position of Silva et al., (2018) is justified by the high P-value (Table 3), which shows that the observed data agrees with the null hypothesis.

Therefore, within the range investigated, the model predictions for HRB, CS, E-MOD and E-BRK are rejected. In Table 4, the statistical significance of independent variables FT and RC on the flexural strength (FS) is further determined. Judging from the low F–value and P-value > 0.05, the firing temperature and residue content do not significantly influence the flexural strength. However, increasing firing temperature and residue content by a square of its original value rejects the null hypothesis and influences the flexural strength.

Table 4: Statistics for ANOVA of the model that describes flexural strength (FS)

Model Term	Regression Coefficient	P-value	F-value
Intercept	-477.7	-	-
RC	0.155	0.483	0.55
FT	0.899	0.057	5.19
RC^2	-0.0021	0.003	19.57
FT^2	-0.0004	0.001	31.91
RC*FT	0.00023	0.39	0.84

$$HRB = 3962 + 11.48RC - 7.46FT - 0.0134RC^2 + 0.00355FT^2 - 0.01035RC \times FT \quad (1)$$

International Journal of Applied Science and Engineering Review

IJASER

ISSN: 2582-6271

Vol. 3, Issue.2, Mar-Apr 2022, page no. 32-43

$$\text{CS (MPA)} = 1473 - 3.48\text{RC} - 2.66\text{FT} + 0.01030\text{RC}^2 + 0.001206\text{FT}^2 + 0.00281\text{RC} \times \text{FT}$$

$$\text{E} - \text{MOD (MPA)} = -4897 - 53.5\text{RC} + 11.1\text{FT} - 0.0718\text{RC}^2 - 0.0061\text{FT}^2 + 0.0521\text{RC} \times \text{FT} \quad (3)$$

$$\text{FS (MPA)} = -477.7 - 0.155\text{RC} + 0.899\text{FT} - 0.002067\text{RC}^2 - 0.000422\text{FT}^2 + 0.000226\text{RC} \times \text{FT} \quad (4)$$

$$\text{E} - \text{BRK (J)} = 1698 - 2.01\text{RC} - 3.16\text{FT} + 0.01759\text{RC}^2 + 0.001479\text{FT}^2 + 0.00117\text{RC} \times \text{FT} \quad (5)$$

Figure 3 shows the XRD graphs of the composite samples with 5.85% and 34.14% representing the highest and lowest residue content considered in this study. From the spectrum shown, the mineralogical phase formed included kaolinite, quartz, albite and illite, indicating the elements contained in the raw materials (kaolin, feldspar and rice husk ash) used. The micrographs shown in Figure 4 present the microstructure transformation from 1030ºC to 1100ºC.

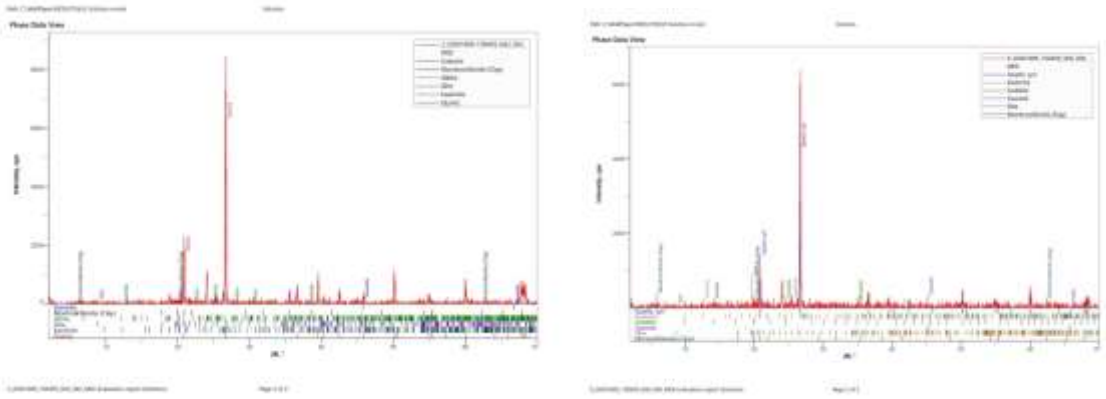

(a) 5.85% RHA **(b) 3.14% RHA**

Figure 3: XRD patterns of samples against % RHA

International Journal of Applied Science and Engineering Review

IJASER

ISSN: 2582-6271

Vol. 3, Issue.2, Mar-Apr 2022, page no. 32-43

It can be observed that as the firing temperature increases towards 1100 ºC, the surface morphology become finer, indicative of improved densification. It is attributed to an increase in the glassy phase, which flows and fills up the open pores leading to reduced porosity in the matrix and shrinkage. This observation agrees with the findings of both Silva et al., (2018) and Gültekin et al., (2017).

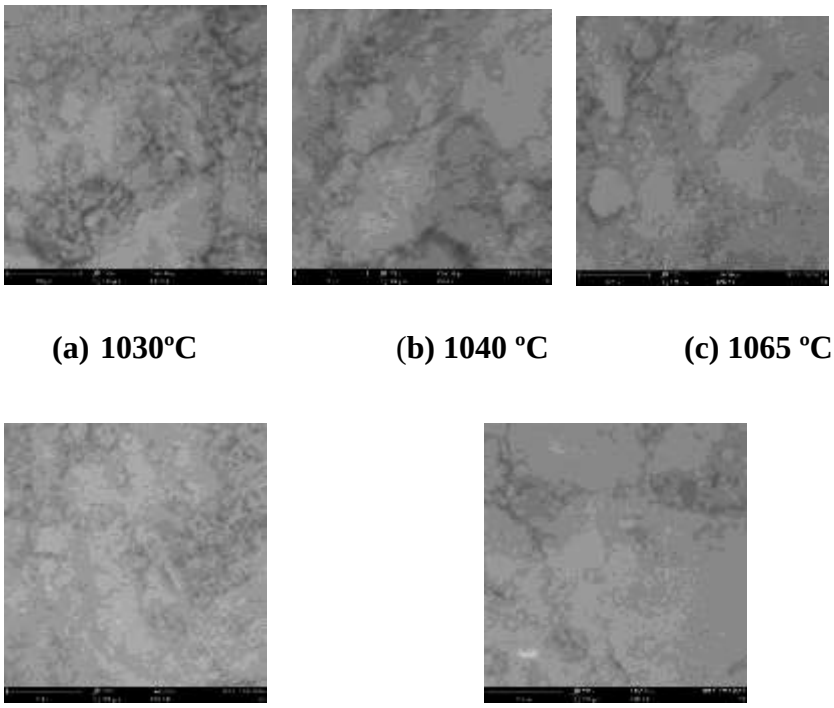

(a) 1030ºC **(b) 1040 ºC** **(c) 1065 ºC**

(d) 1090 ºC **(e) 1100 ºC**

Figure 4: SEM micrograph of fractured surfaces of composites against %RHA

5. CONCLUSION

The application of experimental design was used to determine the appropriateness of the investigated factors (residue content and firing temperature) on the mechanical properties of the rice husk filled ceramic tiles. It was achieved by implementing the central composite design. By applying the design of experiments to evaluate the effect of firing temperature and residue content on the mechanical properties, the ceramic tiles generated a statistically significant effect on flexural strength and energy at the break, judging by the p-value. It means that within the range investigated (1030˚C - 1100˚C), firing temperature and residue content were not influenced by the produced tiles' hardness, compressive strength, and compression modulus. It was attributed to the lack of mullite phase formation within the firing range. However, morphological analysis within the firing range showed that the morphology improved as the

ISSN: 2582-6271

Vol. 3, Issue.2, Mar-Apr 2022, page no. 32-43

firing temperature increased. The mineralogical composition also indicated the effect of the raw materials on the final structure. This research is significant in presenting a systematic and deterministic approach to evaluating and achieving intended product property and quality. However, investigating a higher firing temperature above 1200˚C is recommended.

6. REFERENCES

[1] **Sacks, J.; Welch, W. J.; Mitchell, T. J. and Wynn, H. P. (1989).** Design and Analysis of Computer Experiments. Journal of Statistical Science, Vol. 4, Issue 4, pp. 409–423). https://doi.org/10.1214/ss/1177012413.

[2] **Sundarkrishnaa, K. L. (2015).** Design of experiments. Springer Series in Materials Science, Vol. 171. https://doi.org/10.1007/978-3-319-14069-8_5.

[3] **Abtew, M. A., Kropi, S., Hong, Y., and Pu, L. (2018).** Implementation of Statistical Process Control (SPC) in the Sewing Section of Garment Industry for Quality Improvement. Autex Research Journal, 18(2), 160–172. https://doi.org/10.1515/aut-2017-0034.

[4] **Silva, K. R.; Campos, L. F. A. and De Lima Santana, L. N. (2018).** Use of Experimental Design, to Evaluate the Effect of the Incorporation of Quartzite Residues in Ceramic Mass for Porcelain Tile Production. Materials Research, 22(1), 1–11. https://doi.org/10.1590/1980-5373-MR-2018-0388.

[5] **Ogunbiyi, M. O. (2018).** Optimisation of Parboiling Process using Response Surface Methodology (RSM) to Improve the Physical Properties of Parboiled Milled Rice. International Journal of Engineering Research, Vol. 7(07), 312–318. https://doi.org/10.17577/ijertv7is070117.

[6] **Levinson, W. (2017).** Introduction to Design of Experiments. https://doi.org/10.1002/9780470258354.ch27.

[7] **Abeid S. and Park E. S. (2018).** Suitability of Vermiculite and Rice Husk Ash as Raw Materials for Production of Ceramic Tiles. International Journal of Materials Science and Applications, 7(2), 39. https://doi.org/10.11648/j.ijmsa.20180702.12.

[8] **Chukwudi, B. C.; Ademusuru, P. O. and Okorie, B. A. (2012).** Characterisation of Sintered Ceramic Tiles Produced from Steel Slag. Journal of Minerals and Materials Characterization and Engineering, 2012, 11(09), 863–868. https://doi.org/10.4236/jmmce.2012.119080.

[9] **Quaranta, N.; Caligaris, M.; Unsen, M.; López, H.; Pelozo, G.; Pasquini, J. and Vieira, C. (2014).** Ceramic Tiles Obtained from Clay Mixtures with the Addition of Diverse Metallurgical Wastes. Journal of Materials Science and Chemical Engineering, 02(02), 1–5. https://doi.org/10.4236/msce.2014.2200.

[10] **Correia, S. L.; Dienstmann, G.; Folgueras, M. V. and Segadaes, A. M. (2009).** Effect of Quartz Sand Replacement by Agate Rejects in Triaxial Porcelain, Journal of Hazardous Materials, 163(1),

ISSN: 2582-6271

Vol. 3, Issue.2, Mar-Apr 2022, page no. 32-43

315–322. https://doi.org/10.1016/j.jhazmat.2008.06.094.

[11] **De Silva, G. and Surangi, M. (2017).** Effect of Waste Rice Husk Ash on Structural, Thermal and Run-off Properties of Clay Roof Tiles. Construction and Building Materials, 154(12), 251–257. https://doi.org/10.1016/j.conbuildmat.2017.07.169.

[12] **Haile, E.; Quezon, E. T. and Kebede, G. (2019).** Investigation on the Suitability of Waste Plastic Bottle as Partial Replacement of Sand in a Cement Tile Production. American Journal of Civil Engineering and Architecture, 7(05), 121–127. https://doi.org/10.12691/ajcea-7-3-1.

[13] **Dahiru, T. (2011).** P-Value, a True Test of Statistical Significance? a Cautionary Note. Annals of Ibadan Postgraduate Medicine, 6(1), 21–26. https://doi.org/10.4314/aipm.v6i1.64038.

[14] **Aksel, C. (2003).** The effect of mullite on the mechanical properties and thermal shock behaviour of alumina-mullite refractory materials. Ceramics International, 29(2), 183–188. https://doi.org/10.1016/S0272-8842(02)00103-7.

[15] **Anggono, J. (2005).** Mullite Ceramics: Its Properties Structure and Synthesis, Journal of Mechanical Engineering, 7(1), 1 -10. https://doi.org/10.9744/jtm.7.1.pp.1-10.

[16] **Ban, T. and Okada, K. (1994).** Crystallisation of Mullite and Immiscibility in SiO_2 – Al_2O_3 System. Advanced Materials, 483–486. https://doi.org/10.1016/B978-0-444-819918.50122-9.

[17] **Gültekin E.; Topates G. and Kurama S. (2017).** The Effects of Sintering Temperature on Phase and Pore Evolution in Porcelain Tiles. Ceramics International, 43(14), 11511-11515. http://dx.dpi.org/10.1016/j.ceramint.2017.06.024.